IEEE Access
Multidisciplinary ⋮ Rapid Review ⋮ Open Access Journal

Received 25 November 2023, accepted 5 December 2023, date of publication 12 December 2023,
date of current version 15 December 2023.

Digital Object Identifier 10.1109/ACCESS.2023.3341435

RESEARCH ARTICLE

Delay Dependent Stability Analysis of Load Frequency Control via Asymmetric Lyapunov-Krasovskii Functional

SHREEKANTA KUMAR OJHA AND MADDELA CHINNA OBAIAH
School of Electrical Engineering, Vellore Institute of Technology, Vellore, Tamil Nadu 632014, India
Corresponding author: Maddela Chinna Obaiah (chinna.obaiah@vit.ac.in)

ABSTRACT Time Delays are inevitable in the feedback loops of multi-area load frequency control (LFC), due to the deployment of an open communication network facilitating the transmission of signals from RTU to the control center, and from the center to the grid. Due to the existence of time delays in a communication network, the dynamic performance and stability of the LFC systems are adversely affected. It is necessary to incorporate the effect of time delay in the controller design. This paper focuses on the effects of constant time delays on the multi-area LFC system stability. The stability analysis of LFC subjected to time delays is investigated through the utilization of asymmetric Lyapunov-Krasovskii functional (LKF). Compared with symmetric LKF, asymmetric LKF provides relaxation on the condition that the matrix variables involved in LKF formulation need not be symmetric or positive definite, which provides less the conservativeness on the stability conditions. Further, to reduce the conservativeness, different tightly bounded integral inequalities are utilized in the derivation of stability conditions. By employing asymmetric LKF, two delay-dependent stability criteria are presented in the form of linear matrix inequalities (LMIs) for the systems under study such that an accurate delay margin can be obtained. The LFC system with one and two areas is taken into consideration with a PI controller to validate the efficacy of the proposed stability analysis. The PI controller gains are tuned by analyzing the relationship between PI controller gains and delay margin to balance the dynamic performance and the delay margin of the LFC system. Finally, simulation studies are conducted to validate the efficacy of the suggested methodology.

INDEX TERMS Multi-area load frequency control, PI controller, constant time delay, asymmetric Lyapunov-Krasovskii functional, integral inequalities.

I. INTRODUCTION

Load frequency control (LFC), also known as automatic generation control (AGC), plays a vital role in power system regulation. It is a mechanism that helps to manage the balance between power production and load demand to keep the system frequency uniform within acceptable limits. In an interconnected power grid, changes in load demand or generation can cause frequency deviations, and LFC ensures that these deviations are minimized and the system operates reliably [1], [2]. The LFC systems employ dedicated communication lines to detect and transmit measurement and control signals. The signals are transmitted from RTUs to the control center and the generated control signals are sent to the generating unit. In general, conventional power grids utilize a specialized dedicated communication channel to enable quick measurements and transmission of control signals [3], [4]. In such cases, transmission delay is negligible, often non-existent. Due to the ongoing growth of modern power systems and the increasing trend of power commercialization, it is necessary to transfer pertinent data over the open communication network. The time delays come into the picture when an open communication channel is introduced in the LFC system feedback loop [4]. The issue of time delay commonly arises in the LFC system for several reasons. Firstly, adapting a open communication network to transfer

The associate editor coordinating the review of this manuscript and approving it for publication was Nagesh Prabhu.

control signals. Secondly, the presence of a geographically distributed power area further exacerbates the time delay problem. Additionally, time delays can be induced by cyber-attacks that affect the control signal. Lastly, the integration of distributed generating units and non-conventional sources, as discussed in [5], also introduces time delays in the LFC system.

The time delays caused by communication lines were commonly ignored while analyzing the stability of the LFC system but when transmitting data and control signals through dedicated networks, shorter time delays are considered. According to the report, the communication delays observed in LFC systems can vary between 5 and 15 seconds [6]. Communication delays in a system depend on several factors, some of which include transmission media such as digital microwave links, optical fiber cables, power transmission lines, telephone communication lines, and satellite links [7], distance, bandwidth, network congestion, communication protocol, processing time, error handling, routing complexity, system load, jitter, and latency variation. As a result, the occurrence of communication delays may exhibit random variation within a specific range. With the help of delay margins, we can design an appropriate controller that will maintain the system's stability despite the unpredictability of the delay range. There are multiple approaches available for calculating delay margins to assess the sustainability of delayed dynamical systems. The methods discussed can be classified into two primary categories: (1) Frequency domain or direct technique and (2) Time domain or indirect technique. The primary objective of frequency domain methodologies is to calculate all the purely imaginary roots of the characteristic equation which indicates the marginally stability system. Some of the studies like [8], the stability of generator excitation control with delay is analyzed by the removal of the exponential factor in the characteristic equation. The Schur-Chon approach [9] is utilized to estimate the time delay for AGC systems in [10]. The Rekasius substitution technique is used in [11] to find the maximum delay regarding the small signal stability of the power system. These direct methods can be utilized to evaluate the accurate delay margin by determining the eigenvalues of the total system. The limitation of the above-stated method is that, when the size of the system increases, it becomes time-consuming due to the need for a detailed system model. The implementation of this method is not suitable for analyzing the stability of the system with time-varying delays.

The Lyapunov stability theory and linear matrix inequality(LMIs) techniques are utilized in the indirect time domain approach [12], [13], [14]. The primary objective of the indirect method is to determine the maximum delay with less conservative stability conditions for the given time delay system. The conservativeness of the stability conditions depends on the selection of Lyapunov-Krasovski functional [15], [16] and tightly bound integral inequalities [17], [18]. In power system field, delay-dependent stability analysis studies are being implemented to evaluate the delay margins of the wide-area damping controller [19] and LFC system [20]. In the literature, many researchers have presented several methods for evaluating the stability and stabilization of LFC systems that are subjected to time delays [18], [20], [21], [22], [23], [24], [25], [26]. The study conducted in [20] investigated the characteristics of both one area and multi-area LFC system. The objective was to establish the correlation between delay margins and the gain value of the PI controller by utilizing the standard L-K functional. By the findings presented in reference [20], Zhang et al. [21] conducted a subsequent investigation into the relationship between controller gains and time delays as well as the interaction among various areas by utilizing an augmented functional approach. In [18], a novel augmented function was proposed to overcome the issue of stability in a PI controller-based time-variant delay-dependent LFC system. In [22], a triple integral term augmented LKF is utilized to analyze the multi-area LFC system with time delays. The above-mentioned works in LFC utilize different forms of Lyapunov-Krasovskii functional but all the LKFs are common in one point that is the matrices involved in the formation of LKF are symmetric or positive definite in nature. In [27], it has proven that it is not necessary to utilize all symmetric or positive definite matrices in the LKF formulation to be positive definiteness and it still provides less conservative conditions compared with LKF with all symmetric matrices. Inspired by the seminal work in [27], the current research work, we utilized asymmetric LKF to analyze the stability of the delay-dependent multi-area LFC system. To the best of the knowledge of the authors, no literature exists on the role of asymmetric LKF in the stability analysis of multi-area LFC systems subjected to time delays.

The contribution of this study is to analyze the stability of a multi-area LFC system when subjected to constant time delay in the feedback loop. The criterion proposed in [28] is applied in this study to analyze the stability of the LFC system with constant time delays. The initial step is to formulate the PI controller-based multi-area LFC system as a time delay system to incorporate the time delays in the feedback loop. An asymmetric LKF is utilized to derive less conservation stability criteria for the formulated time delay system. The conservativeness of the criterion is further reduced by utilizing Jensen's inequality [9], Wirtinger's integral inequality (WII) [17] and generalized free matrix-based integral inequality (GFMBII). After determining the delay-dependent stability criteria, the delay margins of the LFC system are calculated. Further, an analysis is conducted to examine the correlation between the delay margin and the gains of the PI controller. The objectives of current research work are as follows:

- Formulation of multi-area LFC system as a time delay system to include the impact of time delays in the feedback loop.
- Obtaining two stability criteria in the LMI form based on asymmetric LKF. Compared with symmetric LKF, asymmetric one provides a less conservative criterion by eliminating the constraint that all the matrices included

in the LKF formulation need to be positive definiteness or symmetric.
- To cope with the cross-terms in the derivative of an asymmetrical LKF, different tightly bound integral inequalities are employed which also makes the solution less conservative.
- To determine the maximum stability region for a given delay, the correlation between delay margin and PI controller gains are obtained using MATLAB/Simulink software.

This paper is structured as follows. The one-area and multi-area LFC systems with constant time delays are described in Section II. Section III presents the primary outcome of the time delay system being examined. Section IV presents a comprehensive case studies and subsequent discussion along with simulation studies are executed to assess the proficiency of the criteria used for validation purposes. Section V provides the concluding section of the paper.

II. DYNAMIC MODEL OF LFC WITH CONSTANT TIME-DELAY

The conventional model of the LFC system has been adapted to analyze the system stability subjected to time delays. In such a linear model, the communication time delay is integrated into the control loop for both one-area and multi-area LFC systems [1], [2], [20]. In this LFC system, components like governors, non-reheat type turbines, and generators, which are represented as first-order transfer functions along with a PI controller, which is currently used in industrial applications. The standard values of system parameters are provided in appendix B.

A. ONE-AREA LFC SCHEME

Figure 1 illustrates a dynamical representation of a one-area LFC system with time delay.

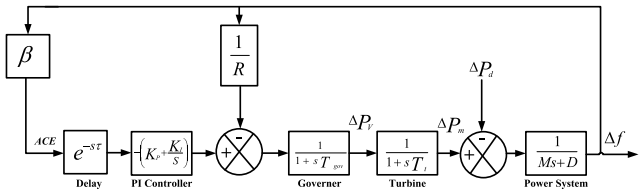

FIGURE 1. Dynamic model of one-area LFC system.

From Figure 1, the state equations of a one-area LFC system can be described as follows:

$$\begin{cases} \Delta\dot{f} = \dfrac{1}{M}\Delta P_m - \dfrac{1}{M}\Delta P_d - \dfrac{D}{M}\Delta f \\ \Delta\dot{P}_m = \dfrac{1}{T_t}\Delta P_v - \dfrac{1}{T_t}\Delta P_m \\ \Delta\dot{P}_v = -\dfrac{1}{R\,T_{gov}}\Delta f - \dfrac{1}{T_{gov}}\Delta P_v \\ \dot{\int} ACE = \beta\,\Delta f \end{cases} \tag{1}$$

The state space representation of the system in Figure 1 is presented as follows: [1], [2]:

$$\begin{aligned} \dot{\acute{x}}(t) &= \acute{A}\acute{x}(t) + \acute{B}\acute{u}(t) + \acute{F}\acute{\omega}(t) \\ \acute{y}(t) &= \acute{C}\acute{x}(t) \end{aligned} \tag{2}$$

where $\acute{x}(t)$, $\acute{y}(t)$, $\acute{u}(t)$, and $\acute{\omega}(t)$ are the vectors of state variables, inputs, outputs, and external disturbances, respectively. The variables of state, output, and disturbance vectors are considered as follows:

$$\begin{aligned} \acute{x}(t) &= \begin{bmatrix} \Delta f & \Delta P_m & \Delta P_v & \int ACE \end{bmatrix}^T \\ \acute{y}(t) &= \begin{bmatrix} ACE & \int ACE \end{bmatrix}^T \\ \acute{\omega}(t) &= \Delta P_d \end{aligned}$$

where, Δf, ΔP_m, ΔP_v, $\Delta P_d, ACE$, and $\int ACE$ are the deviation in frequency, change in mechanical power output, change in position of the steam valve, change in load, area control error and its integral, respectively.

The state matrix ($\acute{A}$), input matrix ($\acute{B}$), output matrix ($\acute{C}$), and disturbance matrix ($\acute{F}$) for the one-area LFC is presented as follows:

$$\acute{A} = \begin{bmatrix} -\frac{D}{M} & \frac{1}{M} & 0 & 0 \\ 0 & -\frac{1}{T_t} & \frac{1}{T_t} & 0 \\ -\frac{1}{RT_{gov}} & 0 & -\frac{1}{T_{gov}} & 0 \\ \beta & 0 & 0 & 0 \end{bmatrix}$$

$$\acute{B} = \begin{bmatrix} 0 & 0 & \frac{1}{T_{gov}} & 0 \end{bmatrix}^T$$

$$\acute{C} = \begin{bmatrix} \beta & 0 & 0 & 0 \\ 0 & 0 & 0 & 1 \end{bmatrix}$$

$$\acute{F} = \begin{bmatrix} -\frac{1}{M} & 0 & 0 & 0 \end{bmatrix}^T$$

where, T_{gov}, T_t, M, D, and R represent the time constants of the governor, the time constant of the turbine, moment of inertia, damping coefficient of the generator, system regulation parameter, respectively. As the one-area LFC system does not include any tie-lines, their will not be any power exchange in this region. Based on that ACE is given by:

$$ACE = \beta\Delta f \tag{3}$$

$\beta = \frac{1}{R} + \mathrm{D}.\ (\beta > 0)$
where, β is termed as frequency bias factor.

In Figure 1, an exponential block $e^{-s\tau}$ is used to represent the delay that occurs in the communication network, where τ represents the constant time delay and it satisfies $0 \le \tau \le \tau_d$. A PI controller is designed for the LFC control system by utilizing ACE as the input signal whose corresponding output signal is shown in equation (4)

$$\acute{u}(t) = -K_P\,ACE - K_I\int ACE \tag{4}$$

where, $K = [K_P\ K_I]$. K_P and K_I denote the proportional and integral gains, respectively.

Due to the communication delay $e^{-s\tau}$, the state equations of the one-area LFC system can be rewritten as follows:

$$\begin{cases} \Delta\dot{f}(t) = \frac{1}{M}\Delta P_m(t) - \frac{1}{M}\Delta P_d(t) - \frac{D}{M}\Delta f(t) \\ \Delta\dot{P}_m(t) = \frac{1}{T_t}\Delta P_v - \frac{1}{T_t}\Delta P_m \\ \Delta\dot{P}_v(t) = -\frac{1}{T_{gov}}K_P\beta\Delta f(t-\tau) - \frac{1}{T_{gov}}K_I\int ACE(t-\tau) \\ -\frac{1}{RT_{gov}}\Delta f(t) - \frac{1}{T_{gov}}\Delta P_v(t) \\ \int ACE = \beta\ \Delta f \end{cases}$$

Based on above equation, the state space representation of the closed-loop LFC system is presented as follows:

$$\begin{cases} \dot{\acute{x}} = \acute{A}\acute{x}(t) + \acute{A}_d\acute{x}(t-\tau) + \acute{F}\Delta P_d\ (t) \\ \acute{y}(t) = \acute{C}\acute{x}(t) \\ \acute{x}(t) = \phi\ (t),\ t \in [-\tau_d,\ 0] \end{cases} \tag{5}$$

where, $\acute{x}(t) \in \mathbb{R}^n$ represents the state vector, $\acute{A} \in \mathbb{R}^{n\times n}$ and $\acute{A_d} \in \mathbb{R}^{n\times n}$ represents the system matrices without and with delay in which $\acute{A_d} = \acute{B}K$, $\acute{B} \in \mathbb{R}^{n\times 1}$ is input matrix and $K \in \mathbb{R}^{1\times n}$ represents the gains of controller. $\phi(t)$ is a continuous vector valued with initial function of $t \in [-\tau_d, 0]$. The system matrices $\acute{A}\acute{x}(t)$ and $\acute{A}_d\acute{x}(t-\tau)$ are represented as follows:

$$\acute{A} = \begin{bmatrix} -\frac{D}{M} & \frac{1}{M} & 0 & 0 \\ 0 & -\frac{1}{T_t} & \frac{1}{T_t} & 0 \\ -\frac{1}{RT_{gov}} & 0 & -\frac{1}{T_{gov}} & 0 \\ \beta & 0 & 0 & 0 \end{bmatrix}$$

$$\acute{A}_d = \begin{bmatrix} 0 & 0 & 0 & 0 \\ 0 & 0 & 0 & 0 \\ -\frac{K_P\beta}{T_{gov}} & 0 & 0 & -\frac{K_P\beta}{T_{gov}} \\ 0 & 0 & 0 & 0 \end{bmatrix}$$

$$\acute{F} = \begin{bmatrix} -\frac{1}{M} & 0 & 0 & 0 \end{bmatrix}^T$$

$$\acute{C} = \begin{bmatrix} \beta & 0 & 0 & 0 \\ 0 & 0 & 0 & 1 \end{bmatrix}$$

B. MULTI-AREA LFC SCHEME

The dynamic model of a power system with multiple areas with an 'n' number of control zones is shown in Figure 2. For simplicity, it is assumed that all generators in a given control area are considered as a single generating unit in a multi-area LFC system. A proportional-integral (PI) controller is implemented in the model as the load frequency controller.

The state-space model of the multi-area LFC system is represented as follows [1], [2].:

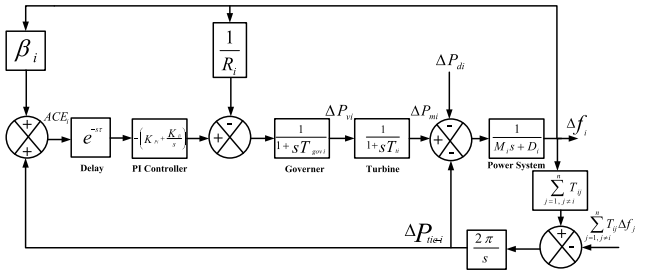

FIGURE 2. Multi area LFC model.

$$\begin{aligned} \dot{\acute{x}}(t) &= \acute{A}\acute{x}(t) + \acute{B}\acute{u}(t) + \acute{F}\acute{\omega}(t) \\ \acute{y}(t) &= \acute{C}\acute{x}(t) \end{aligned} \tag{6}$$

where,

$$\acute{x}_i(t) = \begin{bmatrix} \Delta f_i & \Delta P_{mi} & \Delta P_{vi} & \int ACE_i & \Delta P_{tie-i} \end{bmatrix}^T$$

$$\acute{y}_i(t) = \begin{bmatrix} ACE_i & \int ACE_i \end{bmatrix}^T$$

$$\acute{x}(t) = \begin{bmatrix} \acute{x}_1(t) & \acute{x}_2(t) & \dots & \acute{x}_n(t) \end{bmatrix}^T$$

$$\acute{y}(t) = \begin{bmatrix} \acute{y}_1(t) & \acute{y}_2(t) & \dots & \acute{y}_n(t) \end{bmatrix}^T$$

$$\acute{u}(t) = \begin{bmatrix} \acute{u}_1(t) & \acute{u}_2(t) & \dots & \acute{u}_n(t) \end{bmatrix}^T$$

$$\acute{\omega}(t) = \begin{bmatrix} \Delta P_{d1}(t) & \Delta P_{d2}(t) & \dots & \Delta P_{dn}(t) \end{bmatrix}^T$$

$$\acute{A} = \begin{bmatrix} \acute{A}_{11} & \acute{A}_{12} & \dots & \acute{A}_{1n} \\ \acute{A}_{11} & \acute{A}_{12} & \dots & \vdots \\ \vdots & \vdots & \ddots & \vdots \\ \acute{A}_{n1} & \acute{A}_{n2} & \dots & \acute{A}_{nn} \end{bmatrix}$$

$$\acute{B} = diag\begin{bmatrix} \acute{B}_1 & \acute{B}_2 & \dots & \acute{B}_n \end{bmatrix}$$

$$\acute{C} = diag\begin{bmatrix} \acute{C}_1 & \acute{C}_2 & \dots & \acute{C}_n \end{bmatrix}$$

$$\acute{F} = diag\begin{bmatrix} \acute{F}_1 & \acute{F}_2 & \dots & \acute{F}_n \end{bmatrix}$$

$$\acute{B}_i = \begin{bmatrix} 0 & 0 & \frac{1}{T_{gi}} & 0 & 0 \end{bmatrix}^T$$

$$\acute{F}_i = \begin{bmatrix} -\frac{1}{M} & 0 & 0 & 0 & 0 \end{bmatrix}^T$$

$$\acute{C}_i = \begin{bmatrix} \beta_i & 0 & 0 & 0 & 1 \\ 0 & 0 & 0 & 1 & 0 \end{bmatrix}$$

$$\acute{A}_{ii} = \begin{bmatrix} -\frac{D_i}{M_i} & \frac{1}{M_i} & 0 & 0 & -\frac{1}{M_i} \\ 0 & -\frac{1}{T_{ti}} & \frac{1}{T_{ti}} & 0 & 0 \\ -\frac{1}{R_iT_{govi}} & 0 & -\frac{1}{T_{govi}} & 0 & 0 \\ \beta_i & 0 & 0 & 0 & 1 \\ 2\pi\sum_{j=1,\ j\neq i}^{n} T_{ij} & 0 & 0 & 0 & 0 \end{bmatrix}$$

$$\acute{A}_{ij} = \begin{bmatrix} 0 & 0 & 0 & 0 & 0 \\ 0 & 0 & 0 & 0 & 0 \\ 0 & 0 & 0 & 0 & 0 \\ 0 & 0 & 0 & 0 & 1 \\ -2\pi T_{ij} & 0 & 0 & 0 & 0 \end{bmatrix};\ T_{ij} = T_{ji}.$$

The parameter T_{ij} represents the tie-line synchronization coefficient between the i^{th} and j^{th} control areas of the LFC system.

The ACE in a multi-area LFC system is given as follows:

$$ACE_i = \beta_i \Delta f_i + \Delta P_{tie-i} \tag{7}$$

where, P_{tie-i} represents the net exchange of power between the i^{th} control area. A PI controller-based multi-area LFC system with time delays is presented as follows:

$$\dot{\acute{x}}(t) = \acute{A}\acute{x}(t) + \sum_{i=1}^{n} \acute{A}_{di}\acute{x}(t-\tau_i) + \acute{F}\Delta P_d(t) \tag{8}$$

where,

$$\begin{aligned} \acute{A}_{di} &= diag\begin{bmatrix} 0 & \dots & -\acute{B}_i K_i \acute{C}_i & \dots & 0 \end{bmatrix} \\ K_i &= \begin{bmatrix} K_{Pi} & K_{Ii} \end{bmatrix} \\ K &= diag\begin{bmatrix} K_1 & K_2 & \dots & K_n \end{bmatrix} \end{aligned}$$

The multi-area LFC system incorporates several different time delays. To reduce the computational burden in the analysis process, multiple delays are approximated as a single time delay. The closed-loop multi-area LFC system (8) can be rewritten as follows:

$$\dot{\acute{x}}(t) = \acute{A}\acute{x}(t) + \acute{A}_d\acute{x}(t-\tau) + \acute{F}\acute{\omega}(t) \tag{9}$$

where, $\acute{A}_d = \sum_{i=1}^{n} \acute{A}_{di}$. In a multi-area LFC system, the (9) must be satisfied for the net power exchange over the tie-lines between each control area as follows:

$$\sum_{i=1}^{n} \Delta P_{tie-i} = 0 \tag{10}$$

III. METHODOLOGY FOR STABILITY CRITERION

This section provides the derivation of less conservative stability criterion by utilizing an asymmetric Lyapunov-Krasovskii Functional (LKF) presented in [28] to determine the delay margin τ_d. The different combinations of PI controller gains (such as Proportional (K_P) and Integral (K_I) gains) of the one-area and multi-area LFC systems are chosen to determine the delay margin. The system is said to be asymptotic stable when the delay is less than the delay margin τ_d and the system is said to be unstable when the delay is greater than τ_d. The utilization of asymmetric LKF rather than symmetric LKF reduces the conservativeness of the stability conditions by relaxing the symmetric or positive definite conditions on the matrix variables involved in the LK functional.

Let us consider a time delay system.

$$\begin{aligned} \dot{\acute{x}}(t) &= \acute{A}\acute{x}(t) + \acute{A}_d\acute{x}(t-\tau) \\ \acute{x}(t) &= \theta(t), \forall\, t \in [-\tau, 0] \end{aligned} \tag{11}$$

where $\acute{x}(t) \in \mathbb{R}^n$ represents the state, $\tau > 0$ is the constant time delay by satisfying $0 < \tau < \tau_d$, where τ_d is the upper value of the time delay, and θ(t) implies the initial condition. Here, we will introduce the following lemmas which are useful to derive the less conservative stability conditions by handling the cross terms that arise in the derivative of asymmetric LKF.

Lemma 1 [9]: Given $K > 0$ for any continuous function $\Psi(\omega)$, the following inequality is feasible in $[u_1, u_2] \to \mathbb{R}^n$

$$\begin{aligned} &(u_1,\ u_2)\int_{u_1}^{u_2} \psi^T(\omega)\ K\ \psi\ (\omega)\ d\omega \\ &\geq \left[\int_{u_1}^{u_2} \psi^T(\omega)\ d\omega\right] K \left[\int_{u_1}^{u_2} \psi\ (\omega)\ d\omega\right] \end{aligned} \tag{12}$$

Lemma 2 [17]: Given $K > 0$, for any continuous function $\psi(\omega)$, the following inequality is feasible in $[u_1, u_2] \to \mathbb{R}^n$,

$$\begin{aligned} &\int_{u_1}^{u_2} \psi^T\ (\eta)\ K\ \psi\ (\eta)\ d\eta\ \geq\ \frac{1}{(u_2-u_1)}\left[\int_{u_1}^{u_2} \psi^T(\eta)\ d\eta\right] \\ &K\left[\int_{u_1}^{u_2} \psi\ (\eta)\ d\eta\right] + \frac{3}{(u_2-u_1)}\alpha^T\ K\ \alpha \end{aligned} \tag{13}$$

where,

$$\alpha = \int_{u_1}^{u_2} \psi\ (\eta)\ d\eta\ -\ \frac{2}{(u_2-u_1)}\int_{u_1}^{u_2}\int_{\sigma}^{u_1} \psi\ (\eta)\ d\eta\ d\sigma.$$

Lemma 3 [29]: Let $N \in \mathbb{N}$, $\chi \in \mathbb{R}^n$, and x be a continuous and differential function: $[\alpha, \beta] \to \mathbb{R}^n$. For any matrices $S \in \mathbb{R}^{n\times n} > 0$, $L \in \mathbb{R}^{(N+1)n\times n}$, the following inequality holds:

$$-\int_{\alpha}^{\beta} \dot{x}^T(\theta)S\dot{x}(\theta)d\theta \leq 2\zeta_N^T \Lambda_N^T L\chi + (\beta-\alpha)\chi^T L^T \tilde{S} L\chi \tag{14}$$

where

$$\zeta_N = \begin{cases} \begin{bmatrix} x^T(\beta)\ x^T(\alpha) \end{bmatrix}^T, & N = 0, \\ \begin{bmatrix} x^T(\beta)\ x^T(\alpha)\ \frac{1}{\beta-\alpha}\Theta_0^T\ \cdots\ \frac{1}{\beta-\alpha}\Theta_{N-1}^T \end{bmatrix}^T, & N > 0, \end{cases}$$

$$\Theta_k = \int_{\alpha}^{\beta} F_k(\theta)x(\theta)d\theta$$

$$F_k(\theta) = (-1)^k \sum_{i=0}^{k} \left[(-1)^i \binom{k}{i}\binom{k+i}{i}\right]\left(\frac{\theta-\alpha}{\beta-\alpha}\right)^i,$$

$$\Lambda_N = \begin{bmatrix} \Pi_N^T(0)\ \Pi_N^T(1)\ \cdots\ \Pi_N^T(N) \end{bmatrix}^T,$$

$$\Pi_N(k) = \begin{cases} [I\ \ -I], & N = 0, \\ \begin{bmatrix} I\ (-1)^{k+1}I\ \vartheta_{Nk}^0 I\ \cdots\ \vartheta_{Nk}^{N-1} I \end{bmatrix}, & N \geq 1, \end{cases}$$

$$\vartheta_{Nk}^j = \begin{cases} (2j+1)((-1)^{k+j}-1), & j \leq k, \\ 0, & j > k, \end{cases}$$

$$\tilde{S} = diag\left[\frac{1}{S},\ \frac{1}{3S},\ \cdots\ \frac{1}{(2N+1)S}\right].$$

The delay-dependent stability conditions of one-area and multi-area LFC system are derived based on asymmetric LKF combined with Wirtinger's based inequality and Jensen's inequality in Theorem 1.

Theorem 1: Given $\tau_d > 0$, the system (11) is asymptotically stable if there exist matrices $\hat{M} = \hat{M}^T = \begin{bmatrix} \hat{M}_{11} & \hat{M}_{12} \\ * & \hat{M}_{22} \end{bmatrix} > 0$, $\hat{N} = \begin{bmatrix} \hat{N}_1\ \hat{N}_2 \end{bmatrix}$ with $\hat{N}_1 = \hat{N}_1^T > 0$, $\hat{S}_1 > 0$, and

$\hat{S}_2 > 0$ *such that,*

$$\hat{N} = \begin{bmatrix} \hat{N}_1 + \hat{S}_1 & \frac{1}{2}\hat{N}_2 \\ * & \hat{S}_2 \end{bmatrix} > 0 \tag{15}$$

$$\Delta = \begin{bmatrix} \tau_d\hat{M}_{11} + \tau_d^2\hat{S}_1 & \Delta_{12} & 0 & 0 \\ * & \Delta_{22} & \Delta_{23} & -3\tau_d^{-1}\hat{N}_2 \\ * & * & \Delta_{33} & 6\tau_d^{-2}\hat{N}_2 - 6\tau_d^{-1}\hat{S}_2 \\ * & * & * & 12\tau_d^{-2}\hat{S}_2 \end{bmatrix} > 0 \tag{16}$$

$$\delta = \begin{bmatrix} \delta_{11} & \delta_{12} & \delta_{13} \\ * & \delta_{11} & \delta_{23} \\ * & * & \delta_{33} \end{bmatrix} < 0 \tag{17}$$

where,

$$\begin{aligned}
\Delta_{12} &= \tau_d\hat{M}_{12} + \tau_d\hat{S}_1, \\
\Delta_{22} &= \tau_d\hat{M}_{22} + 4\hat{N}_1 + 4\hat{S}_1, \\
\Delta_{23} &= -6\tau_d^{-1}\hat{N}_1 + 2\hat{N}_2 - 6\tau_d^{-1}\hat{S}_1 \\
\Delta_{33} &= -12\tau_d^{-2}\hat{N}_1 - 3\tau_d^{-1}He(\hat{N}_2) + 12\tau_d^{-2}\hat{S}_1 + 4\hat{S}_2 \\
\delta_{11} &= He(\hat{M}_{11}A + \hat{M}_{12}) + \hat{N}_1 - 4\hat{S}_1 + \tau_d^2A^T\hat{S}_1A + \tau_d^2\hat{S}_2 \\
\delta_{12} &= \hat{M}_{11}A_d - \hat{M}_{12} - 2\hat{S}_1 + \tau_d^2A^T\hat{S}_1A_d \\
\delta_{13} &= A^T\hat{M}_{12} - \hat{M}_{22} + \frac{1}{2}\hat{N}_2^T + 6\tau_d^{-1}\hat{S}_1 \\
\delta_{22} &= -\hat{N}_1 - 4\hat{S}_1 + \tau_d^2A_d^T\hat{S}_1A_d \\
\delta_{23} &= A_d^T\hat{M}_{12} - \hat{M}_{22} - \frac{1}{2}\hat{N}_2 + 6\tau_d^{-1}\hat{S}_1 \\
\delta_{33} &= -12\tau_d^{-2}\hat{S}_1 - \hat{S}_2
\end{aligned}$$

Proof: Choose the asymmetric LKF candidate as

$$U_t = U_{t-1} + U_{t-2} + U_{t-3} \tag{18}$$

where

$$\begin{aligned}
U_{t-1} &= \rho^T(t)\hat{M}\rho(t), \quad \rho(t) = \left[x^T(t)\int_{t-\tau_d}^{t} x^T(\omega)\,d\omega\right]^T \\
U_{t-2} &= \int_{t-\tau_d}^{t} x^T(\sigma)\hat{N}\left[x^T(\sigma)\int_{\sigma}^{t} x^T(\omega)d\omega\right]^T d\sigma \\
U_{t-3} &= \tau_d\int_{t-\tau_d}^{t}\int_{\sigma}^{t}\left[\dot{x}^T(\omega)\hat{S}_1\dot{x}(\omega) + x^T(\omega)\hat{S}_2x(\omega)\right]d\omega d\sigma
\end{aligned}$$

By Lemma 1, $\hat{S}_1 > 0$ and $\hat{S}_2 > 0$, so we obtain

$$\begin{aligned}
&\tau_d\int_{\sigma}^{t}\dot{x}^T(\omega)\hat{S}_1\dot{x}(\omega)d\omega \geq (x(t) - x(\sigma))^T\hat{S}_1(x(t) - x(\sigma)), \\
&\tau_d\int_{\sigma}^{t}x^T(\omega)\hat{S}_2x(\omega)d\omega \geq \left(\int_{\sigma}^{t}x^T(\omega)d\omega\right)\hat{S}_2\left(\int_{\sigma}^{t}x(\omega)d\omega\right)
\end{aligned}$$

Thus, we can infer

$$\begin{aligned}
&U_{t-2} + U_{t-3} \\
&= \int_{t-\tau_d}^{t}\left[x^T(\sigma)\hat{N}\left[x^T(\sigma)\int_{\sigma}^{t}x^T(\omega)d\omega\right]^T\right. \\
&\quad \left.+\tau_d\int_{\sigma}^{t}\left[\dot{x}^T(\omega)\hat{S}_1\dot{x}(\omega) + x^T(\omega)\hat{S}_2x(\omega)\right]d\omega\right]d\sigma \\
&\geq \int_{t-\tau_d}^{t}\begin{bmatrix} x(t) \\ x(\sigma) \\ \int_{\sigma}^{t}x(\omega)d\omega \end{bmatrix}^T\begin{bmatrix} \hat{S}_1 & -\hat{S}_1 & 0 \\ * & \hat{N}_1 + \hat{S}_1 & \frac{1}{2}\hat{N}_2 \\ * & * & \hat{S}_2 \end{bmatrix} \\
&\quad \begin{bmatrix} x(t) \\ x(\sigma) \\ \int_{\sigma}^{t}x(\omega)d\omega \end{bmatrix}d\sigma
\end{aligned} \tag{19}$$

According to (15) and Lemma 2, based on (19) and (16) for (17) we deduce

$$\begin{aligned}
U_t &\geq U_{t-1} + \int_{t-\tau_d}^{t}\begin{bmatrix} \hat{S}_1 & -\hat{S}_1 & 0 \\ * & \hat{N}_1 + \hat{S}_1 & \frac{1}{2}\hat{N}_2 \\ * & * & \hat{S}_2 \end{bmatrix}\begin{bmatrix} x(t) \\ x(\sigma) \\ \int_{\sigma}^{t}x(\omega)d\omega \end{bmatrix}d\sigma \\
&\geq \frac{1}{\tau_d}\eta^T\Delta\eta > 0.
\end{aligned}$$

where

$$\eta^T = \left[x(t), \int_{t-\tau_d}^{t}x(\omega)d\omega, \int_{t-\tau_d}^{t}\int_{\sigma}^{t}x(\omega)d\omega, \int_{t-\tau_d}^{t}\int_{\delta}^{t}\int_{\sigma}^{t}x(\omega)d\omega d\sigma d\delta\right].$$

Time derivative of U_t yields

$$\begin{aligned}
\dot{U}_t &= \dot{U}_{t-1} + \dot{U}_{t-2} + \dot{U}_{t-3} \\
&= 2\dot{\rho}^T(t)\hat{M}\rho(t) + x^T(t)\hat{N}_1x(t) - x^T(t-\tau_d)\hat{N} \\
&\quad \left[x^T(t-\tau_d)\int_{t-\tau_d}^{t}x^T(\omega)d\omega\right]^T + \int_{t-\tau_d}^{t}x^T(\omega)d\omega\hat{N}_2x(t) \\
&\quad + \tau_d^2\dot{x}^T(t)\hat{S}_1\dot{x}(t) - \tau_d\int_{t-\tau_d}^{t}\dot{x}^T(\omega)\hat{S}_1\dot{x}(\omega)d\omega \\
&\quad + \tau_d^2x^T(t)\hat{S}_2x(t) - \tau_d\int_{t-\tau_d}^{t}x^T(\omega)\hat{S}_2x(\omega)d\omega
\end{aligned} \tag{20}$$

Now utilizing Lemma 2 and Lemma 1 to bound

$$-\tau_d\int_{t-\tau_d}^{t}\dot{x}^T(\omega)\hat{S}_1\dot{x}(\omega)d\omega$$

and

$$-\tau_d\int_{t-\tau_d}^{t}x^T(\omega)\hat{S}_2x(\omega)d\omega$$

in (20) respectively. According to 17, we have $\dot{U}_t \leq \chi^T\delta\chi < 0$, where $\chi^T = \left[x^T(t)\,x^T(t-\tau_d)\,\int_{t-\tau_d}^{t}x^T(\omega)d\omega\right]$, the proof is completed. □

Remark 1: Theorem 1, mainly emphasizes on stability conditions of the system. By solving these stability conditions, we can determine maximum delay (delay margin) for which system remains stable. In order to achieve maximum delay margin less conservative stability conditions are derived by using an asymmetric LKF combined with Wintinger-based inequality and Jensen's inequality.

Remark 2: The less conservative delay-dependent stability conditions are obtained by 1) the choice of LKF and 2) the selection of integral inequality to estimate the derivative of the chosen LKF. To reduce the conservativeness in the choice of LKF, an augmented LKF, and a delay-partitioning LKF are mainly employed. The matrices involved in the construction of Lyapunov-Krasovskii Functional are usually positive definite or symmetric ones. In [27], a new technique is developed for

the linear time-delay system stability by relaxing the positive definiteness conditions for the matrices in the LKF and it was ensured that constructed LKF is still symmetric with asymmetric matrix variables in it. In this work, Theorem 1 was developed based on asymmetric LKF (18) for the stability of a multi-area load frequency control system with constant time delays for the first time in this field. The asymmetric LKF in (18) can be reduced to become symmetric by setting $\tilde{N}_2 = 0$ *in Theorem 1. To estimate the derivative of asymmetric LKF, well-known integral inequalities (such as Jensen's inequality (Lemma 1) and Wirtinger's inequality (Lemma 2)) are utilized.*

Remark 3: The utilization of Jensen's inequality, Wirtinger's integer inequality (WII), and Bessel-Legendre inequality [30] to bound the quadratic terms of the integral $\int_{t-\tau_d}^{t} \dot{x}^T(\omega)\hat{S}_1\dot{x}(\omega)d\omega$, *some reciprocally convex terms appears inevitably. Several reciprocally convex inequalities [31], [32] are proposed to handle reciprocally convex terms, but the conservativeness cannot be eliminated by these inequalities. However, these convex terms can be avoided in the derivation of stability conditions by constraining the quadratic term of the integral using the free-matrix-based integral inequality [33]. In the following Theorem, we utilized a generalized free matrix-based inequality (GFMBII) [29] which includes some existing inequalities as special cases to handle the integral term in the derivative of the considered asymmetric LKF in (18).*

The delay-dependent less conservative stability conditions are obtained for one-area and multi-area LFC systems by utilizing asymmetric LKF combined with a generalized free matrix-based integral inequality in the following Theorem.

Theorem 2: Given $\tau_d > 0$, *the system (11) is asymptotically stable if there exist matrices* $\tilde{M} = \tilde{M}^T = \begin{bmatrix} \tilde{M}_{11} & \tilde{M}_{12} \\ * & \tilde{M}_{22} \end{bmatrix} > 0$, $\tilde{N} = \begin{bmatrix} \tilde{N}_1 & \tilde{N}_2 \end{bmatrix}$ *with* $\tilde{N}_1 = \tilde{N}_1{}^T > 0$, $\tilde{S}_1 > 0$, $\tilde{S}_2 > 0$, *and any matrix* L_{ij} $(i = 1, 2, 3, \text{and } j = 1, 2)$ *such that,*

$$\tilde{N} = \begin{bmatrix} \tilde{N}_1 + \tilde{S}_1 & \frac{1}{2}\tilde{N}_2 \\ * & \tilde{S}_2 \end{bmatrix} > 0 \tag{21}$$

$$\Delta = \begin{bmatrix} \tau_d\tilde{M}_{11} + \tau_d^2\tilde{S}_1 & \Delta_{12} & 0 & 0 \\ * & \Delta_{22} & \Delta_{23} & -3\tau_d^{-1}\tilde{N}_2 \\ * & * & \Delta_{33} & 6\tau_d^{-2}\tilde{N}_2 - 6\tau_d^{-1}\tilde{S}_2 \\ * & * & * & 12\tau_d^{-2}\tilde{S}_2 \end{bmatrix} > 0 \tag{22}$$

$$\delta = \begin{bmatrix} \delta_{11} & \delta_{12} & \delta_{13} & L_{11} & L_{12} \\ * & \delta_{11} & \delta_{23} & L_{21} & L_{22} \\ * & * & \delta_{33} & \frac{1}{\tau_d}L_{31} & \frac{1}{\tau_d}L_{32} \\ * & * & * & S_1 & 0 \\ * & * & * & * & 3S_1 \end{bmatrix} < 0 \tag{23}$$

where,

$$\Delta_{12} = \tau_d\tilde{M}_{12} + \tau_d\tilde{S}_1,$$
$$\Delta_{22} = \tau_d\tilde{M}_{22} + 4\tilde{N}_1 + 4\tilde{S}_1,$$
$$\Delta_{23} = -6\tau_d^{-1}\tilde{N}_1 + 2\tilde{N}_2 - 6\tau_d^{-1}\tilde{S}_1$$
$$\Delta_{33} = -12\tau_d^{-2}\tilde{N}_1 - 3\tau_d^{-1}He(\tilde{N}_2) + 12\tau_d^{-2}\tilde{S}_1 + 4\tilde{S}_2$$

$$\delta_{11} = He(\tilde{M}_{11}A + \tilde{M}_{12}) + \tilde{N}_1 + \frac{1}{\tau_d}He(L_{11}) + \frac{1}{\tau_d}He(L_{12}) + \tau_d^2A^T\tilde{S}_1A + \tau_d^2\tilde{S}_2$$
$$\delta_{12} = \tilde{M}_{11}A_d - \tilde{M}_{12} + \frac{1}{\tau_d}L_{21} + \frac{1}{\tau_d}L_{22} - \frac{1}{\tau_d}L_{11} + \frac{1}{\tau_d}L_{12} + \tau_d^2A^T\tilde{S}_1A_d$$
$$\delta_{13} = A^T\tilde{M}_{12} - \tilde{M}_{22} + \frac{1}{2}\tilde{N}_2^T + \frac{1}{\tau_d^2}L_{31} + \frac{1}{\tau_d^2}L_{32} - \frac{2}{\tau_d^2}L_{12}$$
$$\delta_{22} = -\tilde{N}_1 - \frac{1}{\tau_d}He(L_{21}) + \frac{1}{\tau_d}He(L_{22}) + \tau_d^2A_d^T\tilde{S}_1A_d$$
$$\delta_{23} = A_d^T\tilde{M}_{12} - \tilde{M}_{22} - \frac{1}{2}\tilde{N}_2 - \frac{1}{\tau_d^2}L_{31} + \frac{1}{\tau_d^2}L_{32} - \frac{2}{\tau_d^2}L_{22}$$
$$\delta_{33} = -\frac{2}{\tau_d^3}He(L_{32}) - \tilde{S}_2$$

Proof: By utilizing a generalized free matrix-based integral inequality presented in Lemma 3 with $N = 1$ to handle the quadratic term of the integral $\int_{t-\tau_d}^{t} \dot{x}^T(\omega)\hat{S}_1\dot{x}(\omega)d\omega$, and employing the derivation process similar to that of Theorem 1, one can readily obtain Theorem 2. □

Remark 4: Many advanced approaches have been proposed to deal with the time-varying delay system [34], [35], [36] and to investigate the problem of load frequency control [37], [38]. However, the LKF considered in the above references are symmetric ones. In this work, an asymmetric LKF method is combined with integral inequalities to reduce the conservativeness of stability conditions. When this method is further extended to study the LFC system with time-varying delays, an improved inequalities with parameter dependent slack variables [39] will be used rather than constant matrices which can be considered as future work. Further, we believe that the concept of asymmetric matrix variables utilization in the construction of LKF (i.e., asymmetric LKF) could provide less conservativeness by combining the latest integral inequalities.

IV. CASE STUDIES

In this section, we examined the feasibility of the proposed stability analysis on a multi-area LFC system. The parameters of the LFC systems are presented in Appendix B. The upper bound of the constant time delay (i.e., delay margin) of two case studies is calculated by solving the aforementioned stability criteria in the MATLAB/Simulink environment using the LMI toolbox. For a constant time delay ($\mu = 0$), τ_d are evaluated for different combinations of PI controller gains. Further, simulation-based studies are conducted to investigate the effects of time delays on the LFC system.

A. ONE-AREA LFC SCHEME

1) THEORETICAL RESULTS FOR THE DELAY MARGIN

The delay margin is determined through the utilization of various sets of gains for the controller. The gain of K_I in the PI controller is initially examined, as K_P has typically a small magnitude i.e., $K_P = 0$ in a actual LFC system.

The outcomes of the τ_d about the various values of K_I at ($\mu = 0$) are presented in Table 1 and Figure 3. The calculated delay margin by theorem 1 is compared with [20] for delay derivative $\mu = 0$.

TABLE 1. τ_d versus K_I with $\mu = 0$ (One area).

	Proposed Method		
K_I	$\tau_d(s)$ Theorem 1	$\tau_d(s)$ Theorem 2	$\tau_d(s)$ Method [20]
0.05	30.8534	134.9875	27.9268
0.10	15.1729	71.8057	13.775
0.15	9.9420	50.2797	9.0560
0.20	7.3233	40.6366	6.6915
0.40	3.3774	24.8549	3.1241
0.60	2.0403	19.9246	1.9104
1.00	0.9226	16.2347	0.8858

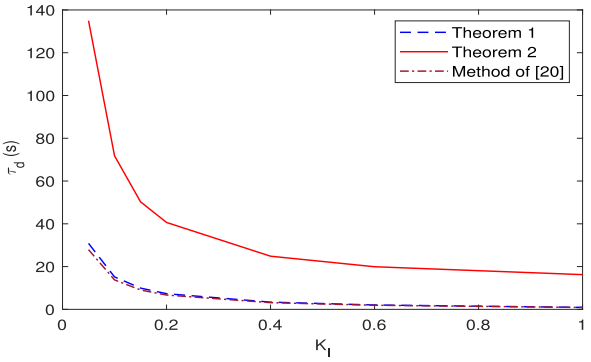

FIGURE 3. Delay margin $\tau_d \propto K_I$ (One-area LFC Scheme, μ=0.)

From Table 1, we can observe that there is a considerable decrease in the delay margin when the values of K_I change from 0.05 to 1.00. It can be noticed that, the delay margin obtained by Theorem 1 is larger when compared to the delay margin of [20]. This shows that, the proposed stability criterion provides more stability to the system. Adding on to it, it can be noticed that when Theorem 2 was used, we obtained more delay margin compared to Theorem 1 and [20].

For different combination of K_P and K_I gains in Theorem 1, the corresponding τ_d values are shown in Table 2 and figure 4. It can be noticed that, for low gains of K_P and K_I we obtained larger delay margin where as a smaller delay margin was obtained for higher gains of K_P and K_I. When K_P was constant, the delay margin decreased for an increase in K_I. When K_I value is less than 0.1, the delay margin increased up to $K_P \leq 0.1$ and later it decreased. Similarly, when K_I value is between 0.15 to 0.6, the delay margin increased until $K_P \leq 0.2$ and later it decreased. Finally when K_I value is 1, the delay margin increased up to $K_P \leq 0.4$ and later it decreased. This pattern of increasing and decreasing of τ_d for various values of K_P and K_I is useful to determines the maximum delay margin. A similar analysis was done with Theorem 2, whose corresponding values are shown in Table 3. From the Table, it can be inferred that, the delay margin was high for lower values of K_P and K_I where as low for high values of K_P and K_I.

TABLE 2. τ_d versus K_I and K_P with $\mu = 0$ (One area).

$\tau_d(s)$	K_I						
K_P	0.05	0.10	0.15	0.20	0.40	0.60	1.00
0.00	30.8534	15.1729	9.9420	7.3233	3.3774	2.0403	0.9226
0.05	31.7509	15.6478	10.2588	7.5610	3.4964	2.1196	0.9699
0.10	32.1393	15.9679	10.5292	7.7763	3.6044	2.1912	1.0118
0.20	31.4551	15.8497	10.6002	7.9289	3.7653	2.3087	1.0777
0.40	26.4963	13.6950	9.3705	7.1604	3.5937	2.2559	1.0966
0.60	19.5697	10.4290	7.2670	5.6109	2.8256	1.7362	0.8924
1.00	0.5945	0.5848	0.5745	0.5636	0.5153	0.4630	0.3608

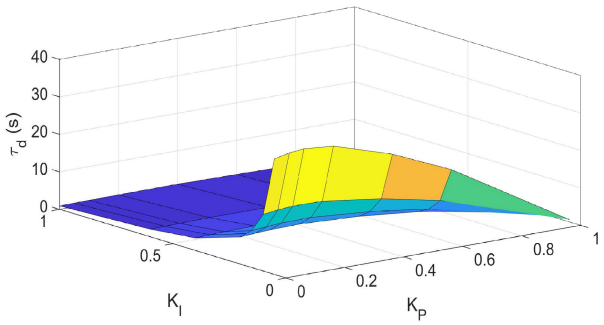

FIGURE 4. Delay margin τ_d (Theorem 1) $\propto K_I$ (One-area LFC Scheme, μ=0.)

TABLE 3. τ_d versus K_I and K_P with $\mu = 0$ (One area).

$\tau_d(s)$	K_I						
K_P	0.05	0.10	0.15	0.20	0.40	0.60	1.00
0.00	134.987	71.805	50.279	40.636	24.854	19.924	16.234
0.05	133.999	71.169	50.439	40.477	24.799	19.898	16.226
0.10	133.069	70.797	49.947	40.310	24.743	19.871	16.217
0.20	131.629	70.059	49.743	39.899	24.629	19.818	16.200
0.40	128.460	68.498	48.685	39.287	24.399	19.711	16.166
0.60	124.569	66.9199	47.827	37.999	24.163	19.601	16.131
1.00	116.797	63.499	45.546	37.133	23.685	19.379	16.059

2) SIMULATION-BASED VERIFICATION OF THEORETICAL DELAY MARGINS

To validate the precision of the theoretical delay margin results obtained by Theorem 1, time-domain simulations are carried out in MATLAB/Simulink. The PI controller gains ($K_P = 0.0, K_I = 0.4$ and $K_P = 0.2, K_I = 0.4$) combinations are considered to evaluate the efficacy of the stability criterion and the correctness of the delay margin. The oscillations are triggered in the system by applying a positive load disturbance ΔP_d with magnitude 0.1 $p.u.$ at time $t = 10$ seconds. The frequency deviation Δf and ACE responses of the one area LFC system are presented in Figure 5 and 6 under various time delays with $K_P = 0.0$ and $K_I = 0.4$, respectively. From the figures, we can observe that the system becomes marginally stable by producing sustained

oscillations for constant delay $\tau = 3.3774s$ which matches with delay margin $\tau_d = 3.3774s$ obtained in Table 2, and larger than the delay margin in [20]. When $\tau\ (= 3.0s) < \tau_d$, the system becomes stable and the responses converge to the equilibrium point asymptotically. When $\tau\ (= 3.6s) > \tau_d$, the system becomes unstable and the responses diverge away to the equilibrium point.

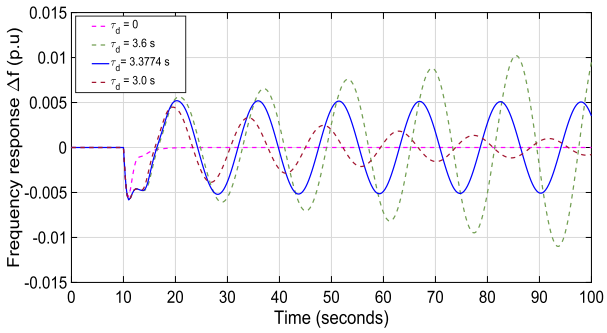

FIGURE 5. Frequency response curve (one area) (K_P=0, K_I=0.4 with $\mu = 0$.)

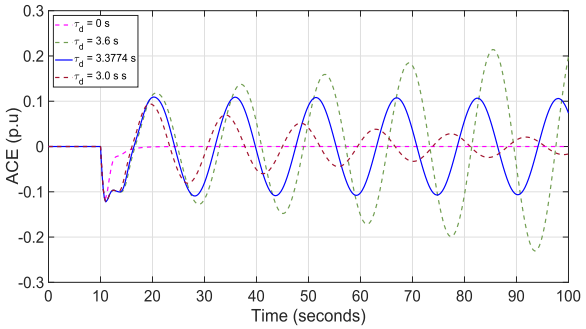

FIGURE 6. ACE response curve of one area. (K_P=0, K_I=0.4 with $\mu = 0$.)

For the gains $K_P = 0.2$ and $K_I = 0.4$, the frequency deviation Δf and ACE responses of one-area LFC system under different delays are shown in Figure 7 and 8, respectively. From the figures, we can observe that the system becomes marginally stable by producing sustained oscillations for constant delay $\tau = 3.7653s$ which matches with delay margin $\tau_d = 3.7653s$ obtained in Table 2, and larger than the delay margin in [20]. Figures also illustrate the stable and unstable operation of the system with delays less than ($\tau = 3.5s$) and more than ($\tau = 3.9s$) the delay margin.

B. TWO-AREA LFC SYSTEM

1) THEORETICAL RESULTS FOR THE DELAY MARGIN

In this section, the delay margin τ_d of the two-area LFC system subjected to constant time delays i.e., ($\mu = 0$) is determined by using Theorem 1 and Theorem 2. Initially, the variation of τ_d was obtained for different values of K_I keeping $K_P(= 0)$ constant is presented in Table 4. The calculated delay margins are compared with Table 4 from the reference [20]. The result shows similar delay margin patterns in both two-area and one-area LFC systems. The value of τ_d decreases as the gain value K_I increases which is shown in

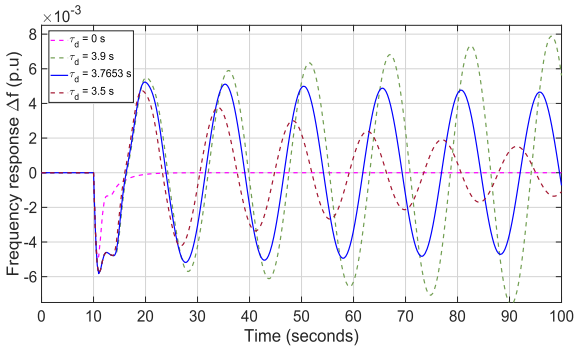

FIGURE 7. Frequency response curve (One area) (K_P=0.2, K_I=0.4 with $\mu = 0$.)

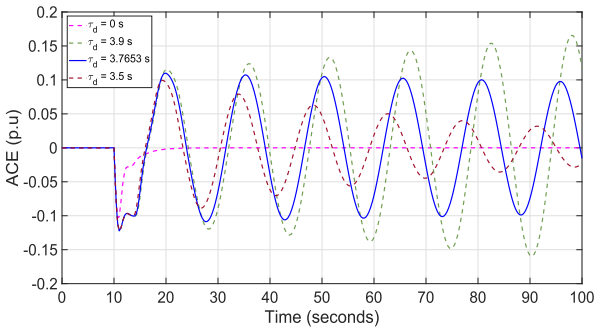

FIGURE 8. ACE response curve (One area) (K_P=0.2, K_I=0.4 with $\mu = 0$.)

Figure 9. Theorem 2 provides a larger delay margin compared to Theorem 1 and reference [20].

TABLE 4. τ_d versus K_I with $\mu = 0$ (Two area).

	Proposed Method		
KI	$\tau_d(s)$ Theorem 1	$\tau_d(s)$ Theorem 2	$\tau_d(s)$ Method [20]
0.05	30.4568	131.9989	27.8484
0.10	15.0720	71.2999	13.6987
0.15	9.8356	50.2490	8.9743
0.20	7.2105	39.7820	6.6026
0.40	3.2311	24.5999	3.0023
0.60	1.8495	19.8777	1.7452
1.00	0.5860	16.2453	0.5725

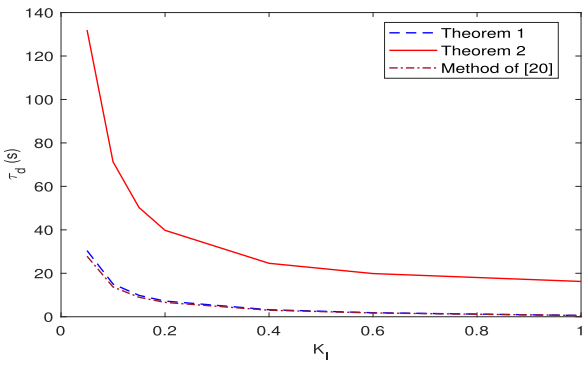

FIGURE 9. Delay margin curve (one-area) ($\tau_d \propto K_I$, $\mu = 0$).

TABLE 5. τ_d versus K_I and K_P with $\mu = 0$ (Two area).

$\tau_d(s)$ / K_P	K_I 0.05	0.10	0.15	0.20	0.40	0.60	1.00
0.00	30.7568	15.0720	9.8356	7.2105	3.2311	1.8495	0.5860
0.05	31.6809	15.5471	10.1525	7.4482	3.4999	1.9283	0.6319
0.10	32.1109	15.9072	10.4342	7.6642	3.4571	1.9984	0.6696
0.20	31.4166	15.8145	10.5698	7.8597	3.6136	2.0997	0.7099
0.40	26.4809	13.6448	9.3226	7.1170	3.4270	1.9553	0.6622
0.60	19.5842	10.4006	7.2329	5.5641	2.3332	1.3107	0.4549
1.00	0.4866	0.4749	0.4628	0.4502	0.3962	0.3996	0.2299

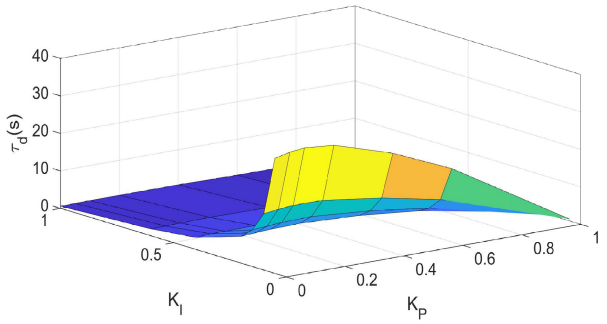

FIGURE 10. Delay margin pattern (Two areas) based on Theorem 1 ($\tau_d \propto K_P, K_I$ with μ=0).

For different values of K_P and K_I, τ_d is calculated based on Theorem 2 and presented in Table 5 and Figure 10. The impacts of controller gains closely resemble those observed in the one-area LFC system. For instance, when the value of K_I is increased by keeping the value of K_P constant, it leads to a decrease in τ_d. In the case of fixed K_I, the influence of K_P on the delay margin exhibited two distinct behaviours. Firstly, when K_I value ranged between 0.05 to 0.1, the τ_d value increased when K_P varied from 0 to 0.1 and later it decreased. Secondly, for a given $K_I \geq 0.15$, the delay margin increased up to $K_P \geq 0.2$ and after that it decreased. Similarly, the delay margin is determined for different values of PI controller gains using Theorem 2 and the values presented in Table 6. From the values it can be observed that, the pattern of increasing and decreasing of delay margin using various PI values are same as Table 3.

2) SIMULATION-BASED VERIFICATION OF THEORETICAL DELAY MARGINS

To examine the correctness of delay margins obtained by Theorem 1, two distinct sets of PI controller gains, i.e., ($K_P = 0$, $K_I = 0.4$) and ($K_P = 0.2$, $K_I = 0.4$) are considered in the simulation. From Table 5, the delay margins associated with this particular set of gains are $\tau_d = 3.2311$ and τ_d =3.6136 respectively. To verify this, it is assumed that the identical positive load disturbance occurred at time t= 10 seconds, with magnitude $\Delta P_{d1} = \Delta P_{d2} = 0.1$ p.u. The response curve of frequency variations and ACE of two area LFC systems with $K_P = 0$, $K_I = 0.4$ are shown in Figure 11 and 12. Based on the response, it can be concluded that the two-area LFC system achieves a moderate level of stability at a delay margin $\tau_d = 3.2311$s and stable when

TABLE 6. τ_d versus K_I and K_P with $\mu = 0$ (Two area).

$\tau_d(s)$ / K_P	K_I 0.05	0.10	0.15	0.20	0.40	0.60	1.00
0.00	131.9989	71.2999	50.2490	39.7820	24.5999	19.8777	16.2453
0.05	130.9867	71.0377	50.0600	39.6139	24.5798	19.8768	16.2269
0.10	128.6039	70.5999	49.8001	39.4688	24.5638	19.8098	16.2348
0.20	123.9541	69.4968	49.4064	39.2033	24.4938	19.8000	16.2242
0.40	116.5992	67.0003	48.4655	38.5919	24.1999	19.7000	16.1855
0.60	109.9788	64.6297	47.2786	37.9700	23.9999	19.5875	16.1700
1.00	96.3564	60.2699	44.8109	36.5295	23.5699	19.3363	16.0950

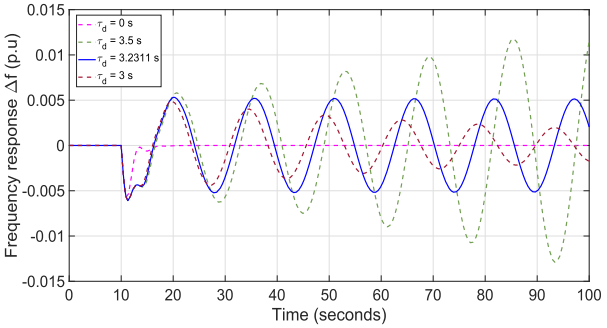

FIGURE 11. Frequency response curve (Two area) ($K_P = 0$, $K_I = 0.4$ with $\mu = 0$.)

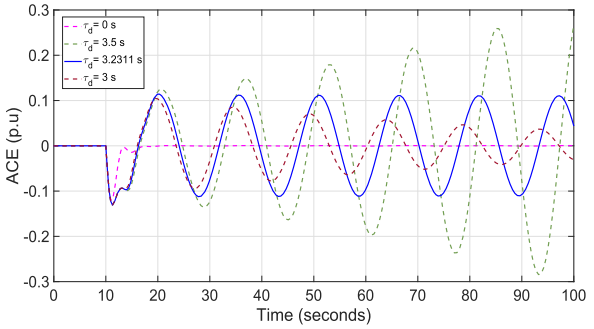

FIGURE 12. ACE response curve (Two area) ($K_P = 0$, $K_I = 0.4$ with $\mu = 0$.)

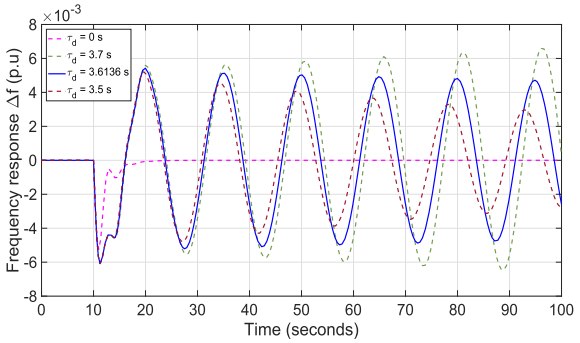

FIGURE 13. Frequency response curve (Two area) ($K_P = 0.2$, $K_I = 0.4$ with $\mu = 0$.)

$\tau < \tau_d$ and becomes unstable when the $\tau > \tau_d$. The Figure 13 and Figure 14 shows the frequency deviation and ACE response curves of the system with gains $K_P = 0.2$ and $K_I = 0.4$. From the responses, we can observe that the two area LFC system becomes marginally stable at a delay

margin $\tau_d = 3.6136$ s and becomes stable and unstable if the time delay is less than or greater than the τ_d, respectively. It is seen that the theoretical delay margin findings exhibit a high degree of agreement with the outcomes acquired through simulations, hence validating the accuracy and efficacy of the suggested methodology.

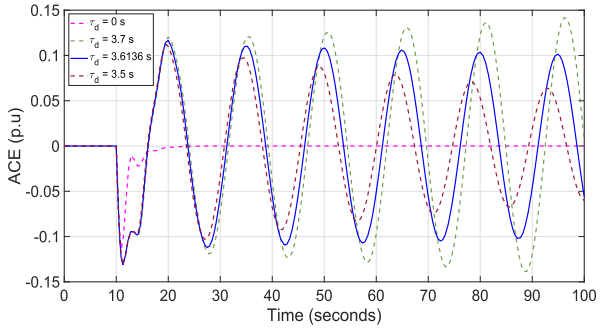

FIGURE 14. ACE response curve (Two area) ($K_P = 0.2$, $K_I = 0.4$ with $\mu = 0$.)

V. CONCLUSION

The paper analyzes the stability of multi-area LFC systems which are influenced by constant time delay caused by the communication networks. A multi-area LFC system with a PI controller has been designed as a time delay system with a constant time delay in the feedback loop. After that, an asymmetric LKF is considered to handle the time delays. By utilizing asymmetric LKF, the reduced conservativeness delay-dependent stability conditions are formulated in LMI form. The conservativeness is further reduced by utilizing different tight bound integral inequalities to handle the integral terms in the derivative of asymmetric LKF. The following observations and remarks are obtained from the theoretical and simulation studies:

1) The PI controller gains play a crucial role in determining the delay margins.
2) When K_P value was maintained constant, the value of τ_d increased with decreasing value of K_I.
3) When K_I was constant, the value of τ_d increased first and then decrease with an increasing values of K_P.
4) Similar τ_d values are obtained form both theoretical and simulations which indicates that the proposed methods can be used in the estimation of delay margins in LFC systems.
5) The results obtained provide a solid evidence that, the proposed methodology is superior to the existing methods in achieving less conservative conditions.

Above findings can be utilised to to appropriately determine the controller gains to ensure stability and achieve the intended damping performance of the multi-area LFC system even in the presence of communication delays. The LKF constructed by the asymmetric matrix variables will provide less conservative conditions compared to the symmetric one. Further this work with latest integral inequalities can be extended for renewable sources integrated LFC and electric vehicle subjected to time-varying delays

APPENDIX A
NOMENCLATURE

Acronym

ACE	Area Control Error.
LFC	Load Frequency Control.
RTU	Remote Terminal Unit.
LMI	Linear Matrix Inequalities.
LKF	Lyapunov-Krasovskii Functional.
WII	Wirtinger's based integral inequalities.
GFMBII	Generalized free matrix based integral inequalities.

Symbols

τ_d	Time delay.
ACE_i	Area control error.
K_{Pi}	Proportional gain.
K_{Ii}	Integral gain.
β_i	Frequency bias coefficients.
R_i	System regulation parameters.
M_i	Moment of Inertia of generator.
D_i	Damping Coefficient of generator.
T_{govi}	Time-constant of Governor in second.
T_{ti}	Time-constant of Turbine in second.
Δf_i	Frequency deviancy.
ΔP_{tie-i}	Deviancy in Tie-line power.
ΔP_{vi}	Change in position of steam valve.
ΔP_{mi}	Turbine generator output.
ΔP_{di}	Change in load.

APPENDIX B
SYSTEM PARAMETER

System Papameters	Area-1	Area-2
R_i	0.5	0.5
D_i	1.0	1.0
β_i	21.0	21.0
$M_i(s)$	10.0	10.0
$T_{govi}(s)$	0.1	0.1
$T_{ti}(s)$	0.3	0.3
$T_{ij}(s)$	0.1968	

REFERENCES

[1] R. Shankar and P. Kundur, *Power System Stability and Control II*. New York, NY, USA: McGraw-Hill, 1994, p. 581.
[2] H. Bevrani, *Robust Power System Frequency Control*, vol. 4. Cham, Switzerland: Springer, 2014.
[3] A. Khalil and A. S. Peng, "An accurate method for delay margin computation for power system stability," *Energies*, vol. 11, no. 12, p. 3466, Dec. 2018.
[4] S. Bhowmik, K. Tomsovic, and A. Bose, "Communication models for third party load frequency control," *IEEE Trans. Power Syst.*, vol. 19, no. 1, pp. 543–548, Feb. 2004.
[5] Z. Hu, S. Liu, W. Luo, and L. Wu, "Resilient distributed fuzzy load frequency regulation for power systems under cross-layer random denial-of-service attacks," *IEEE Trans. Cybern.*, vol. 52, no. 4, pp. 2396–2406, Apr. 2022.

[6] S. Sönmez, S. Ayasun, and C. O. Nwankpa, "An exact method for computing delay margin for stability of load frequency control systems with constant communication delays," *IEEE Trans. Power Syst.*, vol. 31, no. 1, pp. 370–377, Jan. 2016.
[7] B. Naduvathuparambil, M. C. Valenti, and A. Feliachi, "Communication delays in wide area measurement systems," in *Proc. 34th Southeastern Symp. Syst. Theory*, Mar. 2002, pp. 118–122.
[8] K. Walton and J. E. Marshall, "Direct method for TDS stability analysis," *IEE Proc. D, Control Theory Appl.*, vol. 134, no. 2, p. 101, 1987.
[9] K. Gu, J. Chen, and V. L. Kharitonov, *Stability of Time-Delay Systems*. Cham, Switzerland: Springer, 2003.
[10] M. Liu, L. Yang, D. Gan, D. Wang, F. Gao, and Y. Chen, "The stability of AGC systems with commensurate delays," *Eur. Trans. Electr. Power*, vol. 17, no. 6, pp. 615–627, Nov. 2007.
[11] Ş. Sönmez, S. Ayasun, and U. Eminoğlu, "Computation of time delay margins for stability of a single-area load frequency control system with communication delays," *WSEAS Trans. Power Syst.*, vol. 19, p. 21, Jan. 2014.
[12] M. Wu, Y. He, J.-H. She, and G.-P. Liu, "Delay-dependent criteria for robust stability of time-varying delay systems," *Automatica*, vol. 40, no. 8, pp. 1435–1439, Aug. 2004.
[13] W. Wang, M.-H. Liu, H.-B. Zeng, and G. Chen, "Stability analysis of time-delay systems via a Delay-Derivative-Partitioning approach," *IEEE Access*, vol. 10, pp. 99330–99336, 2022.
[14] B. Song, Y. Zhang, J. H. Park, and Z. Yang, "Delay-dependent stability analysis of stochastic time-delay systems involving Poisson process," *J. Franklin Inst.*, vol. 358, no. 1, pp. 1087–1102, Jan. 2021.
[15] C. Hua, Y. Wang, and S. Wu, "Stability analysis of neural networks with time-varying delay using a new augmented Lyapunov–Krasovskii functional," *Neurocomputing*, vol. 332, pp. 1–9, Mar. 2019.
[16] K. Shi, H. Zhu, S. Zhong, Y. Zeng, Y. Zhang, and W. Wang, "Stability analysis of neutral type neural networks with mixed time-varying delays using triple-integral and delay-partitioning methods," *ISA Trans.*, vol. 58, pp. 85–95, Sep. 2015.
[17] A. Seuret and F. Gouaisbaut, "Wirtinger-based integral inequality: Application to time-delay systems," *Automatica*, vol. 49, no. 9, pp. 2860–2866, Sep. 2013.
[18] F. Yang, J. He, and D. Wang, "New stability criteria of delayed load frequency control systems via Infinite-Series-Based inequality," *IEEE Trans. Ind. Informat.*, vol. 14, no. 1, pp. 231–240, Jan. 2018.
[19] Z. Sun, J. Zhao, and H. Long, "Design of a delay dependent wide area damping controller using cyber–physical power system architecture," *Energy Rep.*, vol. 9, pp. 510–517, May 2023.
[20] L. Jiang, W. Yao, Q. H. Wu, J. Y. Wen, and S. J. Cheng, "Delay-dependent stability for load frequency control with constant and time-varying delays," *IEEE Trans. Power Syst.*, vol. 27, no. 2, pp. 932–941, May 2012.
[21] C.-K. Zhang, L. Jiang, Q. H. Wu, Y. He, and M. Wu, "Further results on delay-dependent stability of multi-area load frequency control," *IEEE Trans. Power Syst.*, vol. 28, no. 4, pp. 4465–4474, Nov. 2013.
[22] F. Yang, J. He, J. Wang, and M. Wang, "Auxiliary-function-based double integral inequality approach to stability analysis of load frequency control systems with interval time-varying delay," *IET Control Theory Appl.*, vol. 12, no. 5, pp. 601–612, Mar. 2018.
[23] W. Guo, F. Liu, R. Zou, and K. Liu, "H_∞ load frequency control of power systems with multiple time-varying delays via improved reciprocally convex inequality," *J. Franklin Inst.*, vol. 360, no. 12, pp. 7933–7957, Aug. 2023.
[24] X.-C. Shangguan, Y. He, C.-K. Zhang, L. Jiang, and M. Wu, "Load frequency control of time-delayed power system based on event-triggered communication scheme," *Appl. Energy*, vol. 308, Feb. 2022, Art. no. 118294.
[25] G. Zhang, J. Li, O. Bamisile, Y. Xing, D. Cai, and Q. Huang, "An H_∞ load frequency control scheme for multi-area power system under cyber-attacks and time-varying delays," *IEEE Trans. Power Syst.*, vol. 38, no. 2, pp. 1336–1349, Mar. 2023.
[26] L. Jin, Y. He, C.-K. Zhang, X.-C. Shangguan, L. Jiang, and M. Wu, "Robust delay-dependent load frequency control of wind power system based on a novel reconstructed model," *IEEE Trans. Cybern.*, vol. 52, no. 8, pp. 7825–7836, Aug. 2022.
[27] S. Xu, J. Lam, B. Zhang, and Y. Zou, "New insight into delay-dependent stability of time-delay systems," *Int. J. Robust Nonlinear Control*, vol. 25, no. 7, pp. 961–970, May 2015.
[28] Z. Sheng, C. Lin, B. Chen, and Q.-G. Wang, "Asymmetric Lyapunov–Krasovskii functional method on stability of time-delay systems," *Int. J. Robust Nonlinear Control*, vol. 31, no. 7, pp. 2847–2854, 2021.
[29] H.-B. Zeng, X.-G. Liu, and W. Wang, "A generalized free-matrix-based integral inequality for stability analysis of time-varying delay systems," *Appl. Math. Comput.*, vol. 354, pp. 1–8, Aug. 2019.
[30] A. Seuret and F. Gouaisbaut, "Hierarchy of LMI conditions for the stability analysis of time-delay systems," *Syst. Control Lett.*, vol. 81, pp. 1–7, Jul. 2015.
[31] P. Park, J. W. Ko, and C. Jeong, "Reciprocally convex approach to stability of systems with time-varying delays," *Automatica*, vol. 47, no. 1, pp. 235–238, Jan. 2011.
[32] C.-K. Zhang, Y. He, L. Jiang, M. Wu, and Q.-G. Wang, "An extended reciprocally convex matrix inequality for stability analysis of systems with time-varying delay," *Automatica*, vol. 85, pp. 481–485, Nov. 2017.
[33] H.-B. Zeng, Y. He, M. Wu, and J. She, "Free-matrix-based integral inequality for stability analysis of systems with time-varying delay," *IEEE Trans. Autom. Control*, vol. 60, no. 10, pp. 2768–2772, Oct. 2015.
[34] T.-S. Peng, H.-B. Zeng, W. Wang, X.-M. Zhang, and X.-G. Liu, "General and less conservative criteria on stability and stabilization of T–S fuzzy systems with time-varying delay," *IEEE Trans. Fuzzy Syst.*, vol. 31, no. 5, pp. 1531–1541, May 2023.
[35] H.-B. Zeng, Z.-L. Zhai, and W. Wang, "Hierarchical stability conditions of systems with time-varying delay," *Appl. Math. Comput.*, vol. 404, Sep. 2021, Art. no. 126222.
[36] H.-B. Zeng, Y. He, and K. L. Teo, "Monotone-delay-interval-based Lyapunov functionals for stability analysis of systems with a periodically varying delay," *Automatica*, vol. 138, Apr. 2022, Art. no. 110030.
[37] S.-J. Zhou, H.-B. Zeng, and H.-Q. Xiao, "Load frequency stability analysis of time-delayed multi-area power systems with EV aggregators based on Bessel–Legendre inequality and model reconstruction technique," *IEEE Access*, vol. 8, pp. 99948–99955, 2020.
[38] H.-B. Zeng, S.-J. Zhou, X.-M. Zhang, and W. Wang, "Delay-dependent stability analysis of load frequency control systems with electric vehicles," *IEEE Trans. Cybern.*, vol. 52, no. 12, pp. 13645–13653, Dec. 2022.
[39] W. Wang, H.-B. Zeng, K.-L. Teo, and Y.-J. Chen, "Relaxed stability criteria of time-varying delay systems via delay-derivative-dependent slack matrices," *J. Franklin Inst.*, vol. 360, no. 9, pp. 6099–6109, Jun. 2023.

SHREEKANTA KUMAR OJHA received the bachelor's and master's degrees in electrical engineering from the Biju Patnaik University of Technology, Odisha, in 2003 and 2014, respectively. He is currently pursuing the Ph.D. degree in electrical engineering with the Vellore Institute of Technology, Vellore, Tamil Nadu. He has several years of experience as a Faculty Member with DRIEMS Polytechnic, Odisha. From 2014 to 2022, he was the Head of the Department of Electrical Engineering. He has a profound interest in various areas of specialization within the field of electrical engineering. More specifically, he focuses on power system control, time-delay systems, renewable integration, and optimization techniques.

MADDELA CHINNA OBAIAH received the degree from JNTU Anantapur, India, in 2011, and the master's and Ph.D. degrees in electrical engineering from the National Institute of Technology (NIT), Rourkela, India, in 2014 and 2019, respectively. He is currently an Assistant Professor (Senior) with the School of Electrical Engineering, Vellore Institute of Technology, Vellore. His research interests include power system stability and control, time-delay systems, load frequency control, renewable integration, control of non-linear systems, and actuator saturation.